A Method to Measure and Estimate Normalized Contrast in Infrared Flash Thermography

Ajay M. Koshti, NASA Johnson Space Center, Houston

ABSTRACT

The paper presents further development in normalized contrast processing used in flash infrared thermography method. Method of computing normalized image or pixel intensity contrast, and normalized temperature contrast are provided. Methods of converting image contrast to temperature contrast and vice versa are provided. Normalized contrast processing in flash thermography is useful in quantitative analysis of flash thermography data including flaw characterization and comparison of experimental results with simulation. Computation of normalized temperature contrast involves use of flash thermography data acquisition set-up with high reflectivity foil and high emissivity tape such that the foil, tape and test object are imaged simultaneously. Methods of assessing other quantitative parameters such as emissivity of object, afterglow heat flux, reflection temperature change and surface temperature during flash thermography are also provided. Temperature imaging and normalized temperature contrast processing provide certain advantages over normalized image contrast processing by reducing effect of reflected energy in images and measurements, therefore providing better quantitative data. Examples of incorporating afterglow heat-flux and reflection temperature evolution in flash thermography simulation are also discussed.

Keywords: normalized contrast, flash infrared thermography

1. INTRODUCTION

Flash or pulsed infrared (IR) thermography is a Nondestructive Evaluation (NDE) method used in inspection of thin nonmetallic materials such as laminated composites in the aerospace industry. It is primarily used to detect delamination-like anomalies, although surface cracks are also detectable to some extent. In most circumstances, a single-sided or reflection technique is used where the flash lamp (heat source) and IR camera (detector) are on same side of the test object (part) inspected. Maldague[1] provides general information on flash thermography including practical examples and mathematical analysis. Carslaw and Jaeger[2] provide analytical solutions for thermal conduction in an isotropic material for many cases of heat sources and boundary conditions that are applicable to flash thermography. Spicer[3] provides information on both theory and applications in active thermography for nondestructive evaluation.

2. EQUIPMENT AND TECHNIQUE

Flash thermography equipment consists of a flash-hood, flash power supply/trigger unit, flash duration controller, camera data acquisition electronics and a personal computer (PC). See Fig. 1a. A short duration (e.g. 5 ms), intense (~12 kJ) flash is triggered using a computer keyboard. Data acquisition is triggered a few seconds before the flash and it continues for a set duration. The IR camera provides a digital video or sequence of IR images (or frames) called the datacube of the part surface taken at a chosen frame rate (e.g. 60 Hz). Intensity (gray value) of each pixel in the image is a function of surface temperature of corresponding area on the part at the time of image frame. The flash causes part surface to warm up slightly and the absorbed heat starts to dissipate rapidly. Part surface cools through thermal radiation, convection and conduction. It is assumed that heat conduction within the part is the dominant heat transfer mode until temperature gradients within the part become small. At later times, heat conduction is of the order of combined effect of heat convection and radiation. IR data acquisition and data analysis uses the video data in a short duration immediately after the flash where thermal dissipation is dominated by heat conduction (adiabatic process) within the part. After flash, heat transfer in metallic (high thermal conductivity) and thin non-metallic specimens can be often considered as adiabatic, i.e. convection heat exchange coefficient value can be assumed to be zero in these cases. Limit for considering the adiabatic case for heat transfer is given by expression $Bi = hL/K \leq 0.1$. Here, h is heat convection coefficient, L is specimen thickness, K is specimen thermal conductivity and Bi is the Biot number.

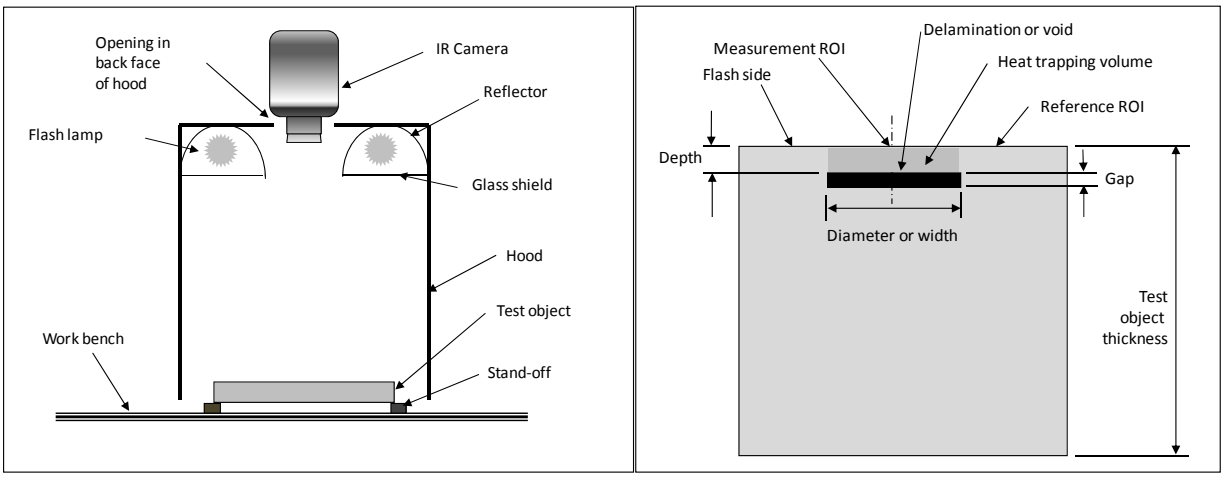

Figure 1. a) Schematic of flash thermography set-up and b) Measurement and reference regions of interest (ROI)

Since flash intensity is approximately uniform over top surface of the plate-like part, heat conduction is in a direction normal to the part surface in most of the area (i.e. area away from edges of the part and flash boundary). Normal to surface heat conduction is obstructed by an anomaly such as a small round gapping delamination as depicted in Fig. 1b. Top surface area surrounding the anomaly cools faster than top surface (footprint) area above the anomaly. IR camera captures the top surface temperature image in terms of pixel intensity (gray value) and shows the anomaly as a hot spot (e.g. an area warmer than surrounding area) which has size and shape of the subsurface anomaly. Relative pixel intensity of the hot spot changes with time. Deeper anomalies appear at later times in the IR video compared to near surface anomalies.

3. DATA ANALYSIS USING COMMERCIAL SOFTWARE

Commercially available IR data analysis software analyzes the IR video data to detect subsurface anomalies by providing enhanced processed images. Commercial software EchoTherm[4] and Mosaic[4] by Thermal Wave Imaging Inc., provide many post-processing options such as, frame subtraction from other frames, frame averaging, pixel intensity rescaling etc. These software also provide first and second derivative images of the pixel intensity with respect to the frame number or time. The derivative images are drawn from fitted data. The fitted data is generated by fitting curves to the pixel intensity versus time decay curve of each pixel. The pixel intensity (average of one or more neighboring pixels) versus time (T-t) curve can be displayed in logarithmic (log-log) scale. An ideal temperature-time decay log-log curve[1] on a thick plate with no anomalies is a straight line with a slope of ~ -0.5. The measured log-log curve on an anomaly would have a constant negative slope for some time after the flash but at a time related to the heat transit time to the anomaly, the decay curve would depart from the linear constant slope (see ASTM E 2582). The departure time or the early appearance time (t_{appear}) can be used to estimate the depth of the anomaly. The software also allows a calibration of a ruler for measuring the distance between the pixels and provides the pixel coordinates. Thermofit Pro[5] also provides many of the above image post-processing routines such as derivatives of pixel intensities. This software also defines a running contrast and normalized contrast. The definition of Thermofit Pro normalized contrast is different than used in this paper. Thermofit Pro software does not define normalized image contrast and the normalized temperature contrast separately and therefore does not make distinction between the two. Both EchoTherm and Thermofit Pro implicitly assume that the pixel intensity is proportional to the surface temperature and is a complete indicator of the surface temperature.

EchoTherm software provides simple pixel "contrast", which is defined as difference in pixel intensity of any two selected areas on the test object surface. ThermoCalc simulation provides simple temperature "contrast" which is defined as the difference in temperature of any two selected areas on the test object surface. The simple contrast evolution looks similar to the normalized contrast, but it is not as useful to correlate to the flaw parameters due to its dependence on flash intensity.

4. ONE DIMENSIONAL CONDUCTION THROUGH THE THICKNESS

In order to develop the subject matter, we begin with basic equations of heat conduction, convection and radiation as they apply to case of flash thermography NDE. Subject matter for this paper comes from US 9,066,028 B1 by the author[14]. Consider a large diameter isotropic flat plate-like test object (part) with top side at temperature T_1 and bottom side at temperature T_2. Heat conduction rate from top to bottom surface across the thickness is given by,

$$q = \frac{T_1 - T_2}{(L/kA)}, \tag{1}$$

$$R_k = \frac{L}{kA}, \tag{2}$$

where,
q = heat conduction rate (cal-s^{-1} or BTU-hr^{-1}),
T_1, T_2 = temperatures in Kelvin (K) or Rankine (°R),
k = thermal conductivity (cal-s^{-1}-°C^{-1}-cm^{-1} or BTU-hr^{-1}-°F^{-1}-ft^{-1}),
A = cross sectional area (cm^2 or ft^2),
L = thickness of the plate (cm or ft), and
R_k = conductive resistance ((s-cal^{-1}-°C or hr-BTU^{-1}-°F).
The above equation is also applicable for heat conduction across a delamination gap with thickness L with one side at temperature T_1 and other at temperature T_2.

5. HEAT TRANSFER FROM A SURFACE DUE TO HEAT CONVECTION

Similarly heat convection across a surface at temperature T_{surf} and ambient temperature T_{amb} is given by,

$$q = \frac{T_{surf} - T_{amb}}{(1/h_{conv}A)}, \text{ and} \tag{3}$$

$$R_h = \frac{1}{h_{conv}A}, \tag{4}$$

where,
q = heat convection rate (cal-s^{-1} or BTU-hr^{-1}),
T_{surf} , T_{amb} = temperatures in Kelvin (K) or Rankine (°R),
h_{conv} = heat convection film coefficient (cal-s^{-1}-°C^{-1}-cm^{-2} or W-K^{-1}-m^{-2}),
A = Surface area (cm^2 or ft^2), and
R_h = convective resistance (s-cal^{-1}-°C or hr-BTU^{-1}-°F).
For natural convection, a typical value for h_{conv} is 4 W-K^{-1}-m^{-2}. Using above equation, heat convection across a uniform delamination air gap with one side at temperature T_1 and other at temperature T_2 ($T_1 > T_2$) is given by,

$$q = \frac{T_1 - T_{amb}}{(1/h_{conv}A)}, \text{ and} \tag{5A}$$

$$q = \frac{T_{amb} - T_2}{(1/h_{conv}A)}. \tag{5B}$$

Ambient temperature of air in the gap is approximately given by,

$$T_{amb} \approx \frac{T_1 + T_2}{2}. \tag{6}$$

In reality, delamination gap thickness is not uniform. The gap thickness tapers to zero at edges of the delamination. When air-gap thickness becomes smaller than threshold thickness given by the Biot number, heat convection across gap is replaced by heat conduction. Heat exchange across boundaries due to convection can be assumed to be zero, if Biot number, $Bi = hL/k \leq 0.1$. This gives an expression for threshold air gap thickness as $L_{thr} = 0.1k/h$. If we take air conductivity to be 0.026 W-m^{-1}-K^{-1} and assume air convection coefficient to be 5 W-m^{-2}-K^{-1}, then a threshold gap thickness of 0.020 inch (0.5 mm) is calculated. For gaps larger than 0.020 inch in thickness, heat convection is the dominant mode of heat transfer in the air gap. Narrowing of air gap results in increased heat conduction across air gap

which manifests as decrease in peak image contrast of the void. Loss of peak image contrast by 20% may not occur until the air-gap narrows significantly compared to the threshold value. Koshti[8-13] provides more information on how delamination air gap thickness relates to normalized peak contrast.

6. HEAT TRANSFER FROM A SURFACE DUE TO HEAT RADIATION

Similarly, heat radiation equations are,

$$q = \frac{T_{surf} - T_{refl}}{\left(1/h_r A\right)}, \tag{7}$$

$$h_r = \varepsilon\sigma\left(T_{surf} + T_{refl}\right)\left({T_{surf}}^2 + {T_{refl}}^2\right), \tag{8}$$

$$R_r = \frac{1}{h_r A}, \tag{9}$$

where,
T_{refl} = apparent temperature experienced by object surface due to camera-side background temperature in Kelvin (K) or Rankine (°R),
T_{amb} = temperature of air surrounding object in Kelvin or Rankine,
σ = Stefan-Boltzmann constant 5.670 400×10^{-8} W·m^{-2}·K^{-4},
ε = emissivity of the test object surface (assume same emissivity on front and rear sides),
R_r = radiative resistance (s-cal^{-1}-°C or hr-BTU^{-1}-°F), and
h_r = heat radiation transfer coefficient (cal-s^{-1}-°C^{-1}-cm^{-2} or BTU-hr^{-1}-°F^{-1}-ft^{-2}). At 300 K, for 10 K difference between object surface temperature and corresponding reflection temperature, the coefficient is less than 6 W-K^{-1}-m^{-2}.
Maximum surface temperature due to flash can be measured using a fast frame rate (frame rate >> 1/flash duration) IR camera and can also be estimated[7]. Koshti[7] introduces concept of threshold thickness in estimating temperature rise due to flash. Change in part thickness does not influence temperature rise if the thicknesses are greater than the threshold thickness. It is important to ensure that the temperature rise is not detrimental to the part.

7. ONE DIMENSIONAL TRANSIENT HEAT TRANSFER

Since, transient heat transfer across thickness of the part is important in flash thermography, transient heat transfer equation in one dimension is given below,

$$\frac{dT}{dt} = \alpha \cdot \frac{d^2T}{dz^2}, \tag{10}$$

where,
T= temperatures in Kelvin (K) or Rankine (°R),
α = test object diffusivity, (cm^2-s^{-1}),
z = coordinate in depth direction, (cm),
t = time, (s).
Initial condition is given by,

$$T(t=0) = T_{in}, \tag{11}$$

where, T_{in} = initial temperature of the test object before flash.
If we neglect air emission, heat flux boundary conditions are given by,

$$-\left(k \cdot \frac{dT}{dz}\right)_{front} = q - h_{front}\left(T_{front} - T_{amb-front}\right) - \sigma\varepsilon\left({T_{front}}^4 - {T_{refl-front}}^4\right), \text{ and} \tag{12}$$

$$\left(k \cdot \frac{dT}{dz}\right)_{rear} = -h_{rear}\left(T_{rear} - T_{amb-rear}\right) - \sigma\varepsilon\left({T_{rear}}^4 - {T_{refl-rear}}^4\right). \tag{13}$$

Heat exchange across part boundaries due to convection can be assumed to be zero provided Biot number is less than or equal to 0.1. Consider an example of ½ cm thick graphite/epoxy plate with k = 0.64 W-m^{-1}-K^{-1}. Using h = 10 W-K^{-1}-m^{-2}, the Biot number is calculated to be 0.078. Therefore, heat conduction is the dominant mode of heat transfer in this example.

8. CAMERA RADIATION MEASUREMENT

In practice, IR camera measures pixel intensity as gray value. Radiometric IR cameras can measure part surface temperature. Currently, radiometric cameras do not compensate for transient surrounding temperature. The radiometric cameras typically have input for a constant surrounding or reflection temperature. They may use a reflective foil to assess steady state reflection temperature. Here, we can use either a radiometric IR camera (i.e. measure apparent temperature) or an IR camera that measures camera irradiance (pixel intensity gray value) and use a technique to capture the transient reflection temperature. We assume that the camera pixel intensity response is proportional to the camera irradiance.

Let us consider a definition of image contrast based on pixel intensity and derive its relationship with part surface temperature. Pixel refers to camera image picture element. Pixel size refers to instantaneous field of view (IFOV), which is corresponding area of object surface imaged in the pixel. If we select a pixel grid area, then the area is called image region of interest (ROI). Size of the ROI then refers to area of object surface imaged in the ROI. Thus, an ROI would contain a grid of pixels. Smallest size of ROI will contain only a single pixel. A single pixel can be referred to as a point. IR camera measures total radiation incident on detector array elements and displays as pixels in the image. Detector element response or pixel intensity registered by the camera is governed by the following equation.

$$W = W_{obj} + W_{refl} + W_{atm}, \tag{14}$$

where, W = pixel intensity due to heat irradiance (W-m^{-2}, cal-s^{-1} cm^{-2}or BTU-hr^{-1} ft^{-2}) of the corresponding camera detector elements measured in gray scale (e.g. 12 bit positive integers). Each of the three terms on right hand side of Eq. (14) are further explained below.

$$W_{obj} = \varepsilon\tau W'_{obj}, \tag{15}$$

$$W_{refl} = (1-\varepsilon)\tau W'_{refl}, \tag{16}$$

$$W_{atm} = (1-\tau)\tau W'_{atm}, \tag{17}$$

where,

W_{obj} = contribution to pixel intensity due to heat emission from corresponding object IFOV,

W_{refl} = contribution to pixel intensity due to heat reflection from corresponding object IFOV and

W_{atm} = contribution to pixel intensity due to heat emission from air between corresponding object IFOV and camera.

If we assume perfect focus and assume that the IFOV has uniform temperature at any time then,

$$W'_{obj} = C_{cam}\sigma T^4, \tag{18}$$

$$W'_{refl} = C_{cam}\sigma T_{refl}^4, \tag{19}$$

$$W'_{atm} = C_{cam}\sigma T_{atm}^4, \tag{20}$$

where,

W'_{obj} = uncompensated contribution to pixel intensity due to heat emission from test object IFOV,

W'_{refl} = uncompensated contribution to pixel intensity due to heat reflection from test object IFOV

W'_{atm} = uncompensated contribution to pixel intensity due to heat emission from the air between the camera and object,

T = surface temperature in Kelvin or Rankine,

T_{refl} = apparent temperature experienced by object surface due to camera-side background temperature in Kelvin or Rankine,

T_{atm} = temperature of air between camera and object in Kelvin or Rankine,

$C_{cam}\sigma$ = camera constant,

ε = thermal emissivity of test object surface, and

τ = thermal radiation (at camera detection wavelength) transmissivity of air between the test object and the camera.

Emissivity is dependent on thermal wavelength for a non-gray or non-black body. Thermal emission wavelength spectrum is affected by the surface temperature. Here, we assume that the emissivity is high and the test object is a gray body such that emissivity is not dependent on the thermal wavelength. However, IR camera measures radiation in a selected band of wavelength (e.g. 3-5 micron). Eq. (18) through Eq. (20) apply to total radiation integrated over all wavelenths. Thus, in Eq. (18) through Eq. (20), which apply to IR cameras, power or exponent of temperature may not be equal to 4. Power of the temperature may be between 2 to 17 depending upon type of IR camera. The following analysis is applicable for these temperature powers.

A calibrated camera provides a linear response for thermal radiation incident on its detector array for a given temperature range. The camera constant is assumed to be constant within a range of 280 K to 350 K. A typical InSb mid-wave camera used in flash thermography operates in infrared wavelength from 3 to 5 micron. Thermal transmissivity of air is a function of distance, humidity, composition of air and thermal wavelength. There is a pronounced dip in air transmissivity at 4.2 micron wavelength due to CO_2 absorption.

Due to short distance (~ 1 ft) between the camera and test object, contribution of air emission (emissivity ~ 0) is very small and is neglected here. Consequently, air transmission (transmissivity ~ 1) is almost 100%. Microbolometer long-wave IR camera works in 9 to12 micron wavelength and has better air transmissivity even for longer distances of several feet (e.g. 30 ft). Therefore, Eq. (14) is simplified to,

$$W \cong W_{obj} + W_{refl} . \tag{21}$$

9. NORMALIZED IMAGE CONTRAST

The paper provides a method of computing normalized image or pixel intensity contrast, and normalized temperature contrast as defined by the author (Koshti[8-14]). It also provides methods of converting image contrast to temperature contrast and vice versa. The subject matter is considered to be part of Koshti[8-14] contrast method. Normalized image contrast is also called normalized irradiance or pixel intensity contrast and is defined by Koshti[8-14] as follows.

$$\bar{C}_w^t = \frac{\Delta W - \Delta W_R}{\Delta W + \Delta W_R} , \tag{22}$$

$$\Delta W = W - W^0 , \tag{23}$$

$$\Delta W_R = W_R - W_R^0 , \tag{24}$$

where,

$\bar{C}_w^t$ = normalized IR image (pixel intensity) contrast,

ΔW = change in pixel intensity of measurement ROI after flash,

W = pixel intensity at the measurement ROI at post flash time t,

W^0 = pixel intensity at the measurement ROI before flash,

ΔW_R = change in pixel intensity of Reference ROI after flash,

W_R = pixel intensity at the reference ROI at post flash time t, and

W_R^0 = pixel intensity at the reference ROI before flash.

10. NORMALIZED TEMPERATURE CONTRAST

The normalized surface temperature contrast is defined by Koshti[8-14] as follows,

$$\bar{C}^t = \frac{\Delta T - \Delta T_R}{\Delta T + \Delta T_R} , \tag{25}$$

$$\Delta T_R = T_R - T_R^0 , \tag{26}$$

$$\Delta T = T - T^0 , \tag{27}$$

where,

$\bar{C}^t$ = normalized flash surface temperature contrast,

ΔT = change in surface temperature of Measurement ROI after flash,

T = surface temperature at the measurement ROI at post flash time t,

T^0 = surface temperature at the measurement ROI before flash,

ΔT_R = surface temperature of reference ROI after flash,

T_R = surface temperature at the reference ROI at post flash time t, and

T_R^0 = surface temperature at the reference ROI before flash.

11. CONVERSION OF NORMALIZED TEMPERATURE CONTRAST TO NORMALIZED IMAGE CONTRAST

Let us investigate how normalized image contrast is related to normalized temperature contrast. As a first approximation, we assume that air transmissivity is unity and air heat radiation is negligible due to short distance (1 ft) between the object and camera. Therefore, the Eq. (14) simplifies to,

$$W \cong \varepsilon W'_{obj} + (1-\varepsilon) W'_{refl} . \tag{28}$$

Substituting, Eq. (18) and Eq. (19) in above equation we get,

$$W \cong C_{cam}\sigma\left(\varepsilon T^4 + (1-\varepsilon)T_{refl}^4\right). \tag{29}$$

Assume that contribution to pixel intensity from reflected temperature remains same as between the measurement ROI and reference ROI. Temperature at a measurement ROI is related to rise in corresponding image ROI pixel intensity by,

$$\Delta W \cong C_{cam}\sigma\left(\varepsilon\left(T^4 - T^{0\,4}\right) + (1-\varepsilon)\left(T_{refl}^4 - T_{refl}^{0\,4}\right)\right) \tag{30}$$

Temperature at a reference ROI is related to rise in the corresponding image ROI pixel intensity by,

$$\Delta W_R \cong C_{cam}\sigma\left(\varepsilon\left(T_R^4 - T_R^{0\,4}\right) + (1-\varepsilon)\left(T_{refl}^4 - T_{refl}^{0\,4}\right)\right) \tag{31}$$

Substituting the above equations in definition of normalized image contrast i.e. Eq. (22) we get,

$$\bar{C}_w^t \cong \frac{\varepsilon\left(\left(T^4 - T^{0\,4}\right) - \left(T_R^4 - T_R^{0\,4}\right)\right)}{\left(\varepsilon\left(\left(T^4 - T^{0\,4}\right) + \left(T_R^4 - T_R^{0\,4}\right)\right) + 2(1-\varepsilon)\left(T_{refl}^4 - T_{refl}^{0\,4}\right)\right)} . \tag{32}$$

If a simulation program is used to generate the temperature evolution at measurement and reference ROIs, then the above expression can be used to compute normalized image contrast provided we estimate reflection temperature evolution. In practice, reflection temperature changes with time due to cooling of flash lamps. Reflected temperature evolution can be estimated based on measured data on a high reflectivity foil and high emissivity tape. Upon estimation of reflected temperature evolution, Eq. (32) can be used to estimate normalized image contrast.

Estimated image contrast would be partially compensated by the reflection temperature. Only camera measurement for reflection temperature is compensated. The reflection temperature evolution has a major contribution from flash lamp radiation. The net heat transfer due to radiation from the flash lamps post flash is very small. In ThermoCalc-3D Pro simulation, heat convection is accounted for. The simulation program provides choices regarding shape and duration of heat pulse. Depending upon user choice, heat source may or may not model the afterglow or the reflection temperature. Thus, if reflection temperature is not modeled in the simulation, then estimation of image contrast from simulated temperature would be considered to be partially compensated for the afterglow.

Alternatively, a second approach is to increase convective heat transfer coefficient by average radiation heat transfer coefficient. In flash thermography, convective heat transfer coefficient is of the order of 5 $W\text{-}K^{-1}\text{-}m^{-2}$. Although radiative heat transfer coefficient is a function of temperature, it is less than 5 $W\text{-}K^{-1}\text{-}m^{-2}$for 10 K difference in temperature at 300 K ambient temperature. The radiative heat transfer coefficient can be lumped together with convective heat transfer coefficient to a value of 10 $W\text{-}K^{-1}\text{-}m^{-2}$ in the simulation. This may allow better prediction of surface temperature in flash thermography using a simulation software and also better prediction of image contrast. A third approach would be to model the heat source as a high intensity pulse followed by a very low intensity decaying afterglow.

12. MEASUREMENT OF PREFLASH TEMPERATURE AND ROI INTENSITY

Estimation of normalized temperature contrast from IR measurement technique requires measurement of preflash surface temperature and measurement of radiation intensity of black tape affixed to surface of the test object. We apply a high emissivity (> 0.95) tape (i.e. 3M 33 or 3M Scotch Brand 235) tape to the test object. See Fig. 2. We measure preflash surface temperature of an ROI in center of the black tape using a calibrated radiometric IR camera. The part surface temperature needs to be close to an equilibrium. We also measure the tape ROI intensity. Assuming high transmissivity of air,

$$W_{tape} = C_{cam}\sigma\left(\left(1-\varepsilon_{tape}\right)T_{refl}{}^{4} + \left(\varepsilon_{tape}\right)T_{tape}{}^{4}\right). \tag{33}$$

Due to high emissivity of the tape, we can write the above equation as,

$$W_{tape} \cong C_{cam}\sigma\left(\varepsilon_{tape}T_{tape}^{4}\right). \tag{34}$$

If we measure preflash tape temperature, then we can estimate the camera constant ($C_{cam}^{'}$) using the following equation.

$$C_{cam}^{'} = C_{cam}\sigma \cong \frac{W_{tape}^{0}}{\varepsilon_{tape}T_{tape}^{0\ 4}} \tag{35}$$

Thus, if preflash tape temperature and preflash tape ROI intensity are measured, then the camera constant can be estimated. We will derive a more precise expression for the camera constant later.

13. ESTIMATION OF REFLECTION TEMPERATURE EVOLUTION USING FOIL-TAPE METHOD

In order to measure reflection temperature evolution, T_{refl} or contribution to pixel intensity due to heat reflection, W_{refl}, we introduce a diffused high reflectivity (> 0.95) reflector such as an aluminum foil that is adequately wrinkled to diffuse the reflection. The foil is placed close to physical location of measurement and reference ROIs, preferably on the test object surface. We can use two foils, on either side of the measurement ROI. See Fig. 2. Here we assume that, reflection temperature is uniform over the test object and foil. Reflection ROI temperature and pixel intensity are related by,

$$W_{foil} = C_{cam}\sigma\left(\left(1-\varepsilon_{foil}\right)T_{refl}{}^{4} + \varepsilon_{foil}T_{foil}{}^{4}\right). \tag{36}$$

Contribution of foil emission to foil pixel intensity is very small compared to foil reflected radiation.
From Eq. (36), we can write an expression for reflection temperature as,

$$T_{refl}{}^{4} \cong \frac{W_{foil} - W_{tape}^{0}\left(\frac{\varepsilon_{foil}}{\varepsilon_{tape}}\right)\left(\frac{T_{foil}{}^{4}}{T_{tape}^{0\ 4}}\right)}{C_{cam}^{'}\left(1-\varepsilon_{foil}\right)}. \tag{37}$$

Also, we can assume that foil temperature is about same as preflash reference temperature due to contact with the test object. Since the black tape is in contact with the part,

$$T_{foil} \cong T_{foil}^{0} \cong T_{R}^{0} \cong T_{tape}^{0}. \tag{38}$$

Therefore, Eq. (37) simplifies to,

$$T_{refl}{}^{4} \cong \frac{W_{foil} - W_{tape}^{0}\left(\frac{\varepsilon_{foil}}{\varepsilon_{tape}}\right)}{C_{cam}^{'}\left(1-\varepsilon_{foil}\right)}. \tag{39}$$

Preflash reflection temperature is given by,

$$T_{refl}^{0\ 4} \cong \frac{W_{foil}^{0} - W_{tape}^{0}\left(\frac{\varepsilon_{foil}}{\varepsilon_{tape}}\right)}{C_{cam}^{'}\left(1-\varepsilon_{foil}\right)}. \tag{40}$$

Difference between fourth power of the reflection temperature before and after the flash is given by,

$$T_{refl}{}^4 - T_{refl}^{0\ 4} \cong \frac{W_{foil} - W_{foil}^0}{C'_{cam}\left(1-\varepsilon_{foil}\right)}. \tag{41}$$

Knowing preflash surface temperature of the tape that is close to ambient, the above expression can be evaluated as a function of time and then substituted in image contrast expression of Eq. (32). Use of the high reflectivity foil and high emissivity tape for computing surface temperature during flash thermography is referred to as the "Foil-Tape Method" here.

14. ESTIMATION OF IMAGE CONTRAST FROM SURFACE TEMPERATURE EVOLUTION DATA

Surface temperature evolution data can be obtained using a simulation program such as ThermoCalc3D. Flash thermography data acquisition using a radiometric camera that accounts for the transient reflection temperature can provide the surface temperature evolution data. However, this feature is not commercially available in radiometric IR cameras currently. Here, we provide an IR measurement method so that this feature can be added to the IR radiometric cameras. Let us define change in foil ROI pixel intensity as,

$$\Delta W_{foil} = W_{foil} - W_{foil}^0 \tag{42}$$

Following normalized image contrast equation is derived from Eq. (32), Eq. (40) and Eq. (41).

$$\bar{C}_w^t \cong \frac{\varepsilon\left(\left(T^4 - T^{0\,4}\right) - \left(T_R^4 - T_R^{0\,4}\right)\right)}{\left(\varepsilon\left(\left(T^4 - T^{0\,4}\right) + \left(T_R^4 - T_R^{0\,4}\right)\right) + 2\dfrac{(1-\varepsilon)\Delta W_{foil}}{C'_{cam}\left(1-\varepsilon_{foil}\right)}\right)} \tag{43}$$

We seek to derive a simpler expression for normalized image contrast. Eq. (30) can be rewritten by factoring as,

$$\Delta W = C_{cam}\sigma\left[\varepsilon(T-T^0)\left(T+T^0\right)\left(T^2+T^{0^2}\right) + (1-\varepsilon)(T_{refl}-T_{refl}^0)\left(T_{refl}+T_{refl}^0\right)\left(T_{refl}^2+T_{refl}^{0\ 2}\right)\right]. \tag{44}$$

For reference ROI, Eq. 31 is written as,

$$\Delta W_R = C_{cam}\sigma\left[\varepsilon(T_R-T_R^0)\left(T_R+T_R^0\right)\left(T_R^2+T_R^{0^2}\right) + (1-\varepsilon)(T_{refl}-T_{refl}^0)\left(T_{refl}+T_{refl}^0\right)\left(T_{refl}^2+T_{refl}^{0\ 2}\right)\right], \tag{45}$$

$$\Delta W - \Delta W_R = C_{cam}\sigma\left[\varepsilon(T-T^0)\left(T+T^0\right)\left(T^2+T^{0^2}\right) - \varepsilon(T_R-T_R^0)\left(T_R+T_R^0\right)\left(T_R^2+T_R^{0^2}\right)\right], \text{ and} \tag{46}$$

$$\Delta W + \Delta W_R = C_{cam}\sigma\left[\varepsilon(T-T^0)\left(T+T^0\right)\left(T^2+T^{0^2}\right) + \varepsilon(T_R-T_R^0)\left(T_R+T_R^0\right)\left(T_R^2+T_R^{0^2}\right) + 2(1-\varepsilon)(T_{refl}-T_{refl}^0)\left(T_{refl}+T_{refl}^0\right)\left(T_{refl}^2+T_{refl}^{0\ 2}\right)\right]. \tag{47}$$

If we assume that difference between the reference and measurement temperature is small (e.g. 5 K) at the time of maximum contrast, then it can be shown that,

$$\left(T+T^0\right)\left(T^2+T^{0^2}\right) \cong \left(T_R+T_R^0\right)\left(T_R^2+T_R^{0^2}\right). \tag{48}$$

Therefore, it can be shown that,

$$\frac{\Delta W - \Delta W_R}{\Delta W + \Delta W_R} \cong \frac{\left[\varepsilon(T-T^0) - \varepsilon(T_R-T_R^0)\right]}{\left[\varepsilon(T-T^0) + \varepsilon(T_R-T_R^0) + 2\left(1-\varepsilon\right)\left(T_{refl}-T_{refl}^0\right)\right]}. \tag{49}$$

Using Eq. (22) and simplifying, the above equation is written as,

$$\bar{C}_W^t \cong \frac{\varepsilon\left(\Delta T - \Delta T_R\right)}{\left[\varepsilon\left(\Delta T + \Delta T_R\right) + 2\left(1-\varepsilon\right)\Delta T_{refl}\right]}, \tag{50}$$

where,

$$\Delta T_{refl} = \left(T_{refl} - T_{refl}^0\right). \tag{51}$$

Rearranging Eq. (50), we can write,

$$\bar{C}_W^t \cong \frac{\left(\Delta T - \Delta T_R\right)}{\left[\left(\Delta T + \Delta T_R\right) + 2\left(\dfrac{1}{\varepsilon} - 1\right)\Delta T_{refl}\right]}. \tag{52}$$

Using definition of the temperature contrast we get,

$$\overline{C}_W^t \cong \frac{\overline{C}^t}{\left[1+\frac{2\left(\frac{1}{\varepsilon}-1\right)\Delta T_{refl}}{\left(\Delta T+\Delta T_R\right)}\right]}. \tag{53}$$

Rearranging the previous equation we get,

$$\overline{C}^t \cong \left[1+\frac{2\left(\frac{1}{\varepsilon}-1\right)\Delta T_{refl}}{\left(\Delta T+\Delta T_R\right)}\right]\overline{C}_W^t. \tag{54}$$

Thus, using Eq. (53) and Eq. (54), normalized image contrast and normalized temperature contrast can be approximately converted from one to the other. We define an expression for the emissivity-power factor ε' as,

$$\varepsilon' \cong \frac{1}{\left[1+\frac{2\left(\frac{1}{\varepsilon}-1\right)\Delta T_{refl}}{\left(\Delta T+\Delta T_R\right)}\right]}, \text{ such that} \tag{55}$$

$$\overline{C}_W^t \cong \varepsilon'\overline{C}^t. \tag{56}$$

The emissivity-power factor indicates that reflection temperature rise, temperature rise and emissivity affect conversion between the two contrasts. Reflection temperature is influenced by heat emitted by glass shield of flash lamps and flash lamps. A low percentage (estimated < 50%) of flash energy in the form of visible light comes through glass shield of the flash lamps during the flash duration. The remaining energy comes as thermal radiation from the glass shield as flash lamps continue to glow after the flash providing apparent increase in the reflection temperature. Glass casing of the bulb and glass shield get hot during flash and continue to provide thermal emission. Some hood designs use fans to cool the lamps after flash reducing their afterglow. If we assume that the reflection temperature is same as ambient temperature such that a shutter covers flash lamps immediately after the flash, then we can simplify the above equation as,

$$\overline{C}^t \cong \overline{C}_W^t. \tag{57}$$

In practice, ΔT_{refl} is positive and image contrast and temperature contrast would differ unless the object has emissivity value of 1. Let us derive equations to compute temperatures needed in temperature contrast using measured ROI intensities. Temperature at a measurement point is given by,

$$T = \left(\frac{\varepsilon_{tape}\frac{W}{W_{tape}^0}T_{tape}^{0\ 4} - (1-\varepsilon)T_{refl}^{\ 4}}{\varepsilon}\right)^{0.25}. \tag{58}$$

In this equation, all quantities are known or measured except the reflection temperature. It is given by Eq. (39) as,

$$T_{refl}^{\ 4} \cong \frac{W_{foil} - W_{tape}^0\left(\frac{\varepsilon_{foil}}{\varepsilon_{tape}}\right)}{\frac{W_{tape}^0}{T_{tape}^{0\ 4}}\left(\frac{1-\varepsilon_{foil}}{\varepsilon_{tape}}\right)}. \tag{59}$$

Preflash temperature at a measurement point is given by,

$$T^0 = \left(\frac{\varepsilon_{tape}\frac{W^0}{W_{tape}^0}T_{tape}^{0\ 4} - (1-\varepsilon)T_{refl}^{0\ 4}}{\varepsilon}\right)^{0.25}. \tag{60}$$

In this equation, all quantities are known or measured except the preflash reflection temperature. It is given by Eq. (40) as,

$$T_{refl}^{0\ 4} \cong \frac{W_{foil}^{0} - W_{tape}^{0}\left(\frac{\varepsilon_{foil}}{\varepsilon_{tape}}\right)}{\frac{W_{tape}^{0}}{T_{tape}^{0\ 4}}\left(\frac{1-\varepsilon_{foil}}{\varepsilon_{tape}}\right)}. \tag{61}$$

Similarly, temperature at reference ROI is given by,

$$T_R = \left(\frac{\varepsilon_{tape}\frac{W_R}{W_{tape}^{0}} T_{tape}^{0\ 4} - (1-\varepsilon) T_{refl}^{4}}{\varepsilon} \right)^{0.25}. \tag{62}$$

Similarly, preflash temperature at reference ROI is given by,

$$T_R^0 = \left(\frac{\varepsilon_{tape}\frac{W_R^0}{W_{tape}^{0}} T_{tape}^{0\ 4} - (1-\varepsilon) T_{refl}^{0\ 4}}{\varepsilon} \right)^{0.25}. \tag{63}$$

Using Eq. (58) through Eq. (63) and Eq. (25), we can compute the temperature contrast. Thus, normalized temperature contrast can be calculated using ROI intensity provided by an IR camera.

15. ESTIMATION OF TEST OBJECT EMISSIVITY

Accuracy of estimation of temperature contrast from measured IR intensity data is very sensitive to value of surface emissivity of the test object. Here, we assume that emissivity of the measurement ROI and reference ROI are same. We can either independently measure emissivity or use a recommended value. Here is another approach to determine emissivity from flash thermography data taken using the foil and tape method. Let us start with a relationship between pixel intensity and temperature for the foil and tape. Using Eq. (39) and Eq. (40) we can write,

$$W_{foil}^{0} = C_{cam}\sigma\left((1-\varepsilon_{foil}) T_{refl}^{0\ 4} + \varepsilon_{foil} T_{tape}^{0\ 4}\right), \text{ and} \tag{64}$$

$$W_{tape}^{0} \cong C_{cam}\sigma\left(\varepsilon_{tape} T_{tape}^{0\ 4} + (1-\varepsilon_{tape}) T_{refl}^{0\ 4}\right). \tag{65}$$

Rearrange the previous two equations and we get,

$$\frac{W_{tape}^{0}}{(1-\varepsilon_{tape})} \cong C_{cam}\sigma\left(\frac{\varepsilon_{tape} T_{tape}^{0\ 4}}{(1-\varepsilon_{tape})} + T_{refl}^{0\ 4}\right), \text{ and} \tag{66}$$

$$\frac{W_{foil}^{0}}{(1-\varepsilon_{foil})} = C_{cam}\sigma\left(T_{refl}^{0\ 4} + \frac{\varepsilon_{foil} T_{tape}^{0\ 4}}{(1-\varepsilon_{foil})}\right). \tag{67}$$

Combine the two equations as follows and rearrange.

$$\frac{W_{tape}^{0}}{(1-\varepsilon_{tape})} - \frac{W_{foil}^{0}}{(1-\varepsilon_{foil})} = C_{cam}\sigma\left(\frac{\varepsilon_{tape} T_{tape}^{0\ 4}}{(1-\varepsilon_{tape})} - \frac{\varepsilon_{foil} T_{tape}^{0\ 4}}{(1-\varepsilon_{foil})}\right), \tag{68}$$

$$\frac{W_{tape}^{0}}{(1-\varepsilon_{tape})} - \frac{W_{foil}^{0}}{(1-\varepsilon_{foil})} = C_{cam}\sigma\left(\frac{\varepsilon_{tape}}{(1-\varepsilon_{tape})} - \frac{\varepsilon_{foil}}{(1-\varepsilon_{foil})}\right) T_{tape}^{0\ 4}, \text{ and} \tag{69}$$

$$C_{cam}^{'} T_{tape}^{0\ 4} = C_{cam}\sigma T_{tape}^{0\ 4} = \frac{\left(\frac{W_{tape}^{0}}{(1-\varepsilon_{tape})} - \frac{W_{foil}^{0}}{(1-\varepsilon_{foil})}\right)}{\left(\frac{\varepsilon_{tape}}{(1-\varepsilon_{tape})} - \frac{\varepsilon_{foil}}{(1-\varepsilon_{foil})}\right)}. \tag{70}$$

Eq. (70) provides a more precise expression for the camera constant in Eq. (35). Rearranging the Eq. (64) and Eq. (65) we get,

$$\frac{W_{tape}^{0}}{\varepsilon_{tape}} \cong C_{cam}^{'}\left(T_{tape}^{0\ 4} + \frac{\left(1-\varepsilon_{tape}\right)T_{refl}^{0\ 4}}{\varepsilon_{tape}} \right), \text{ and} \tag{71}$$

$$\frac{W_{foil}^{0}}{\varepsilon_{foil}} = C_{cam}^{'}\left(\frac{\left(1-\varepsilon_{foil}\right)T_{refl}^{0\ 4}}{\varepsilon_{foil}} + T_{tape}^{0\ 4} \right). \tag{72}$$

Combining Eq. (71) and Eq. (72), we get,

$$\frac{W_{tape}^{0}}{\varepsilon_{tape}} - \frac{W_{foil}^{0}}{\varepsilon_{foil}} \cong C_{cam}\sigma\left(\frac{\left(1-\varepsilon_{tape}\right)T_{refl}^{0\ 4}}{\varepsilon_{tape}} - \frac{\left(1-\varepsilon_{foil}\right)T_{refl}^{0\ 4}}{\varepsilon_{foil}} \right). \tag{73}$$

Combining Eq. (69) and Eq. (73), we get,

$$\frac{\left(\frac{W_{tape}^{0}}{\varepsilon_{tape}} - \frac{W_{foil}^{0}}{\varepsilon_{foil}} \right)}{\left(\frac{W_{tape}^{0}}{\left(1-\varepsilon_{tape}\right)} - \frac{W_{foil}^{0}}{\left(1-\varepsilon_{foil}\right)} \right)} \cong \frac{\left(\frac{\left(1-\varepsilon_{tape}\right)}{\varepsilon_{tape}} - \frac{\left(1-\varepsilon_{foil}\right)}{\varepsilon_{foil}} \right)}{\left(\frac{\varepsilon_{tape}}{\left(1-\varepsilon_{tape}\right)} - \frac{\varepsilon_{foil}}{\left(1-\varepsilon_{foil}\right)} \right)} \frac{T_{refl}^{0\ 4}}{T_{tape}^{0\ 4}}, \text{ and} \tag{74}$$

$$\frac{\left(\frac{W_{tape}^{0}}{\varepsilon_{tape}} - \frac{W_{foil}^{0}}{\varepsilon_{foil}} \right)}{\left(\frac{W_{tape}^{0}}{\left(1-\varepsilon_{tape}\right)} - \frac{W_{foil}^{0}}{\left(1-\varepsilon_{foil}\right)} \right)} \cong -\frac{\left(1-\varepsilon_{tape}\right)}{\varepsilon_{tape}} \frac{\left(1-\varepsilon_{foil}\right)}{\varepsilon_{foil}} \frac{T_{refl}^{0\ 4}}{T_{tape}^{0\ 4}}. \tag{75}$$

Rearrange Eq. (75) and let us define a quantity A as,

$$A = \frac{T_{refl}^{0\ 4}}{T_{tape}^{0\ 4}} = \frac{\left(\frac{W_{tape}^{0}}{\varepsilon_{tape}} - \frac{W_{foil}^{0}}{\varepsilon_{foil}} \right)}{\left(\frac{W_{tape}^{0}}{\left(1-\varepsilon_{tape}\right)} - \frac{W_{foil}^{0}}{\left(1-\varepsilon_{foil}\right)} \right)\left(-\frac{\left(1-\varepsilon_{tape}\right)}{\varepsilon_{tape}} \frac{\left(1-\varepsilon_{foil}\right)}{\varepsilon_{foil}} \right)}. \tag{76}$$

Let us define quantity B as,

$$B = \frac{\left(\frac{W_{tape}^{0}}{\left(1-\varepsilon_{tape}\right)} - \frac{W_{foil}^{0}}{\left(1-\varepsilon_{foil}\right)} \right)}{\left(\frac{\varepsilon_{tape}}{\left(1-\varepsilon_{tape}\right)} - \frac{\varepsilon_{foil}}{\left(1-\varepsilon_{foil}\right)} \right)} \text{ and} \tag{77}$$

$$B = C_{cam}^{'} T_{tape}^{0\ 4}. \tag{78}$$

Camera constant is given by,

$$C_{cam}^{'} = \frac{\left(\frac{W_{tape}^{0}}{\left(1-\varepsilon_{tape}\right)} - \frac{W_{foil}^{0}}{\left(1-\varepsilon_{foil}\right)} \right)}{\left(\frac{\varepsilon_{tape}}{\left(1-\varepsilon_{tape}\right)} - \frac{\varepsilon_{foil}}{\left(1-\varepsilon_{foil}\right)} \right)} \frac{1}{T_{tape}^{0\ 4}}. \tag{79}$$

Preflash temperature at measurement ROI is given by,

$$W^{0} \cong C_{cam}\sigma\left(\varepsilon T^{0^4} + (1-\varepsilon)T_{refl}^{0\ 4} \right). \tag{80}$$

Due to contact of the tape with the test object and assuming steady state of surface temperature and reflection temperature that do not differ more than 5 K from the test object temperature before flash, we can assume that,

$$T^0 \cong T^0_{tape} \tag{81}$$

Substituting Eq. (81) in Eq. (80) we get,

$$W^0 \cong C_{cam}\sigma\left(\varepsilon T^{0\ 4}_{tape} + (1-\varepsilon)T^{0\ 4}_{refl}\right), \tag{82}$$

$$W^0 \cong C_{cam}\sigma T^{0\ 4}_{tape}\left(\varepsilon + (1-\varepsilon)\frac{T^{0\ 4}_{refl}}{T^{0\ 4}_{tape}}\right), \tag{83}$$

$$W^0 \cong B\left(\varepsilon + (1-\varepsilon)A\right), \text{ and} \tag{84}$$

$$\varepsilon \cong \frac{\frac{W^0}{B} - A}{1-A}. \tag{85}$$

Thus, test object emissivity at room temperature can be estimated. This technique, however requires that the tape and foil emissivities are accurately known.

16. EXAMPLE 1: ESTIMATE NORMALIZED TEMPERATURE CONTRAST FROM FLASH THERMOGRAPHY DATA

This example illustrates converting normalized image contrast from thermography data to normalized temperature contrast using additional measurements required for computing reflection temperature. The test object is a plate with back drilled elongated flat bottom slots or holes. Fig. 2 shows a selected IR image of the test object from the flash thermography video data. We have chosen center slot for measurement. Locations of measurement and reference ROI are indicated in Fig. 2. One piece of wrinkled aluminum foil is placed on left side of the test object and second piece of wrinkled aluminum foil is placed on right side of the test object. Locations of the foil ROIs are indicated in Fig. 2. A high emissivity adhesive tape is affixed at top of the test object. Tape ROI is indicated in Fig. 2. Image frame time is close to the peak contrast time. The image indicates pixel intensity in gray scale. Image display contrast is adjusted by using image display adjustment area indicated by a rectangle in dashed line. See Fig. 2.

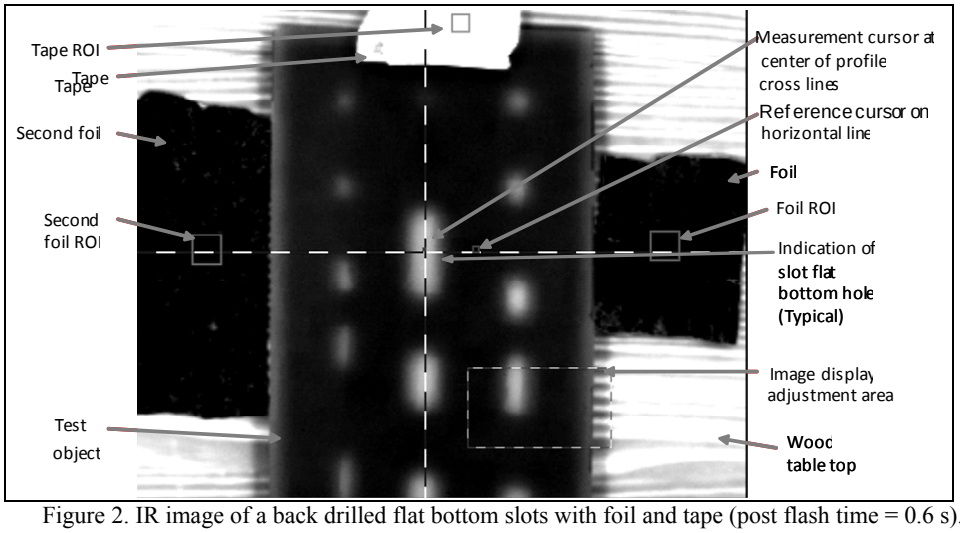

Figure 2. IR image of a back drilled flat bottom slots with foil and tape (post flash time = 0.6 s).

Here, the measurement ROI is a single pixel (0.023 in. x 0.023 in.) and sizes of other ROIs are given below.

Table 1. ROI pixel sizes (1 x 1 pixel = 0.023 in. x 0.023 in.)

ROI	Size
Measurement	1 x 1
Reference	3 x 3
Foil 1 and Foil 2	15 x 15
Tape	9 x 9

Cross lines in Fig. 2 are used to plot pixel intensity along the lines to locate peak intensity points and baseline intensity for selection of measurement and reference ROIs. Fig. 3 shows pixel intensity plot along the horizontal dashed line.

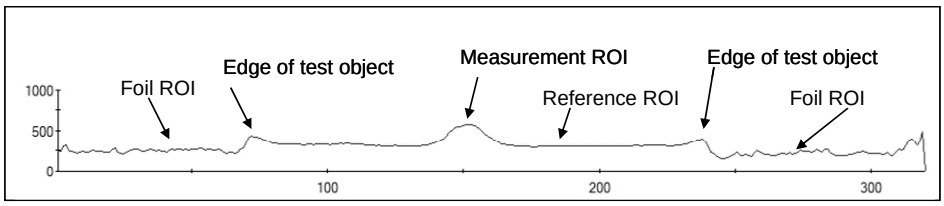

Figure 3. Pixel intensity evolution along a horizontal line (0.6 s).

Table 2 gives preflash measurements and emissivity inputs. Note that Eq. (85) is applied to Table 2 data except for test object emissivity. The test object emissivity is estimated to be 0.75 with single point measurement. We need many such measurements to improve confidence in the value. Therefore, we would use an emissivity value of 0.78 which is published in literature for the test object material.

Table 2: Preflash measurements and emissivity inputs.

T^0_{refl}, K	300
T^0_{tape}, K	296
ε_{tape}	0.99
ε_{foil}	0.05
ε	0.78
W^0_{tape}, gray value	6382
W^0_{foil} (average gray value)	6768.3
W^0_R, gray value	6480

Fig. 4 indicates pixel intensity of the two foil ROIs. The foils are very reflective but specular reflectivity is undesirable as the test object is diffusively reflective. The two foils provide two independent measurements of reflection intensity evolution. The two intensity evolutions agree with each other and an average value is used. The two foils are on either side of the measurement and reference ROIs. Thus, averaging the two foil intensity evolutions probably provides a better estimate of foil intensity evolution as opposed to choosing a single foil intensity evolution.

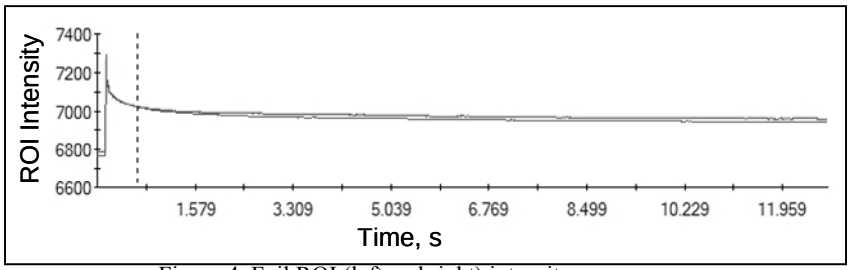

Figure 4. Foil ROI (left and right) intensity.

Fig. 5 shows pixel intensity evolution on the tape. Flash duration is set to 0.003 s. Time between image frames is 0.017 s for a frame rate of 60 frames per second. Tape pixel intensity decays very rapidly before the first post flash frame is captured. The test object reaches maximum temperature at end of the flash duration but the camera is incapable of capturing corresponding peak intensity due to slow frame rate. Fig. 5 indicates that temperature rise is higher than that on the foil. Tape ROI is in area of tape overhang and indicates similar intensity evolution as that of the foil ROI.

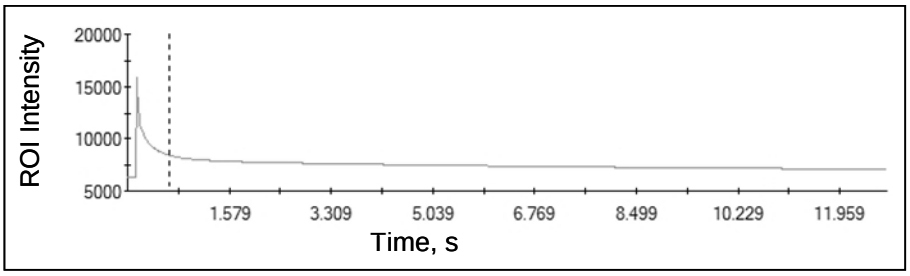

Figure 5. Tape ROI intensity.

Fig. 6 indicates intensity evolution at measurement and reference ROIs.

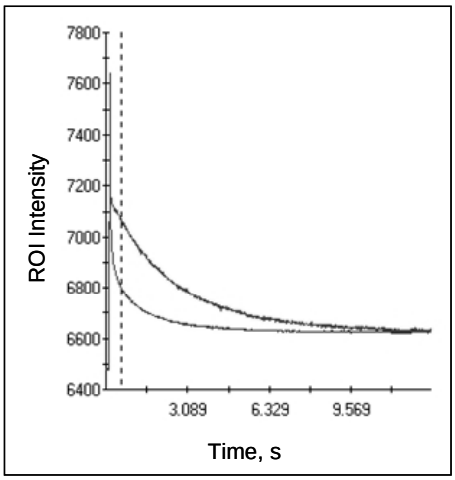

Figure 6. Intensity for measurement (upper) and reference (lower) ROIs.

Fig. 7 indicates simple image contrast which is defined as difference between intensities of measurement and reference ROIs.

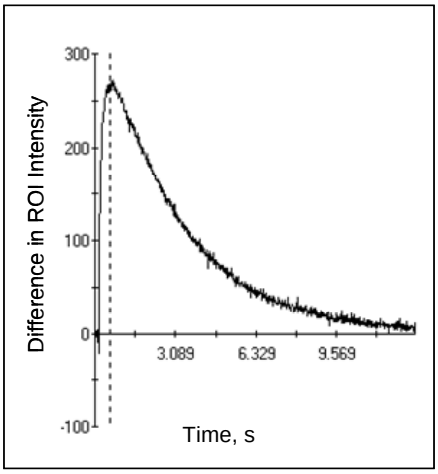

Figure 7. Simple contrast at measurement ROI (peak time 0.5s).

We use Eq. (70) to compute camera constant. Then we use Eq. (39) to compute reflection temperature evolution. See Fig. 8 for plot of the reflection temperature.

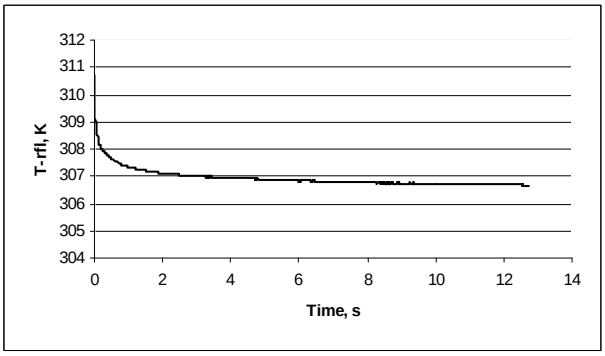

Figure 8. Computed reflection temperature evolution.

Preflash reflection temperature is estimated to be 305 K which is 5 K above preflash temperature of the test object. Also the reflection temperature is a couple of Kelvin higher than the preflash reflection temperature. The data acquisition setup was used to acquire five other shots within 5 minutes before the shot used in this analysis. Thus, the flash lamps and lamp shield became warmer than normal and caused the reflection temperature to be higher than ambient. We use Eq. (58) to compute measurement temperature evolution and Eq. (62) to compute the reference temperature evolution. The three estimated temperature evolutions are displayed in Fig. 9.

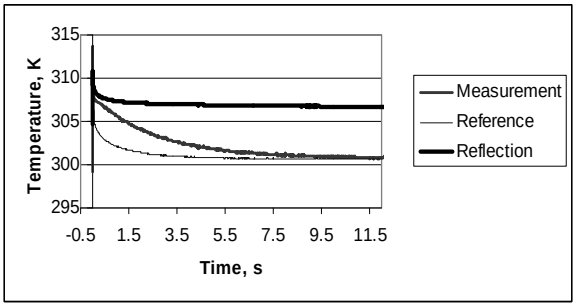

Figure 9. Estimated temperature evolutions at reflection (upper curve), measurement (middle curve), and reference (lower curve) ROIs.

Fig. 10 shows normalized image contrast computed using pixel intensity and $1/4^{th}$ power of pixel intensity to illustrate Eq. (48), which implies that normalized contrast computed with fourth power of temperature and the one computed with unity power of temperature are approximately same.

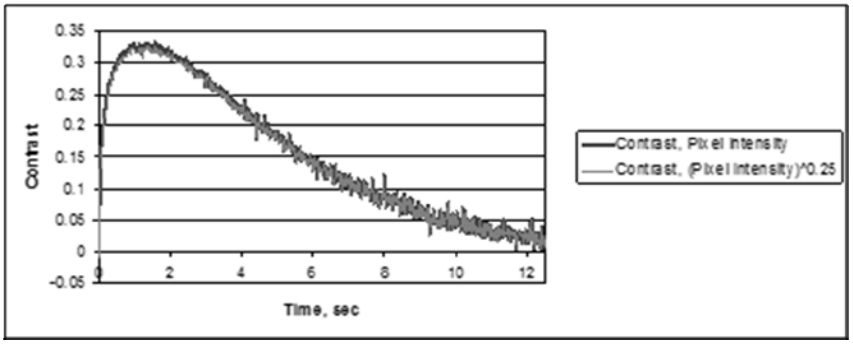

Figure 10. Image contrast computed using pixel intensity (black) and $1/4^{th}$ power of pixel intensity (gray).

Fig. 11 shows estimated temperature contrast evolution along with the image contrast evolution.

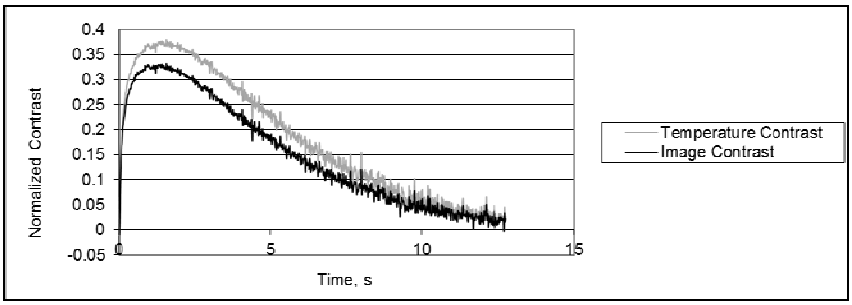

Figure 11. Measured normalized image contrast and estimated normalized temperature contrast (e = 0.78).

Fig. 12 shows the implementation of computing temperature contrast within the IR Contrast software.

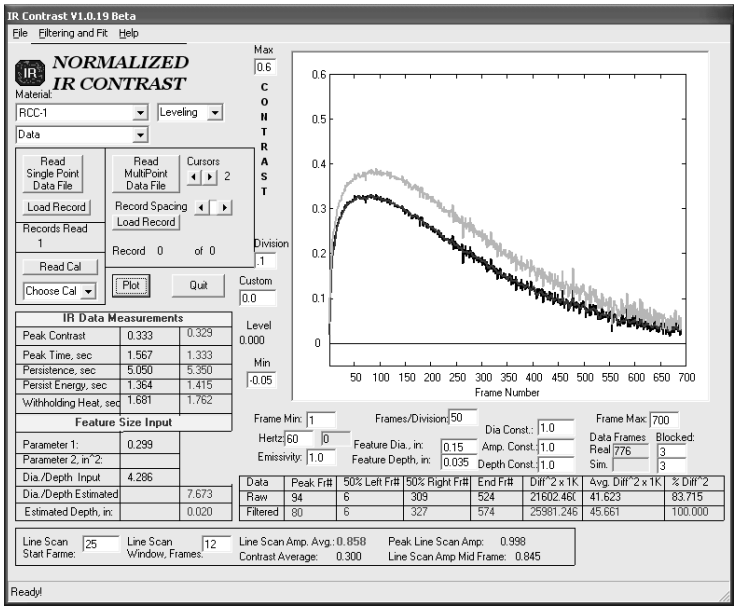

Figure. 12. Temperature contrast (upper curve) and image contrast (lower curve) computed using application.

Fig. 13 shows plot of emissivity-power factor ε'. Two plots are shown. One plot is using approximate Eq. (55). The other plot is ratio of two contrast evolutions from Fig. 12. The plots differ slightly for earlier times but agree well at later times. Emissivity-power factor is approximately same as part emissivity for longer times when change in temperature is very slow with time.

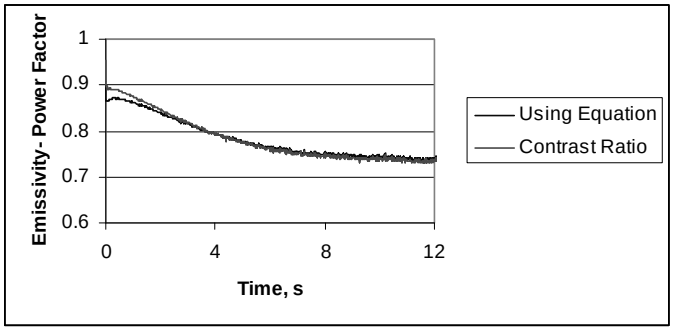

Figure 13. Emissivity-power factor, lower curve using equation and upper curve using contrast ratio.

17. EXAMPLE 2: ESTIMATE IMAGE CONTRAST FROM SIMULATED TEMPERATURE EVOLUTION DATA

Let us estimate normalized image contrast based on Thermo-calc surface temperature simulation results, in order to understand effect of reflection temperature on pixel contrast evolution. We take sample simulation temperature evolution at measurement and reference areas. The simulation power input is 1.8E6 W-m^{-2} with duration of 0.003 s. This assumes about 30% efficiency of converting electrical power (14 kJ source) to absorbed energy. This value is not validated. Depending upon flash power setting, reflection temperature evolution is affected. Here, we only intend to demonstrate effect of reflection temperature evolution. We estimate the reflection temperature evolution based on experimental method explained earlier. See Fig. 14.

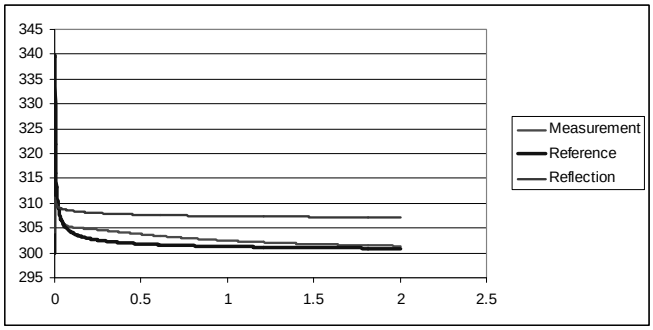

Figure 14. Simulated temperature evolutions with assumed reflection temperature evolution. Reflection temperature (upper curve), measurement temperature (middle curve), and reference temperature (lower curve).

Normalized temperature contrast is calculated using Eq. (25). The results are shown in Fig. 15. Using Eq. (29), pixel intensity can be determined if camera constant is known. Let us assume test object emissivity to be 0.78. Using Eq. (32) we can compute the image contrast.

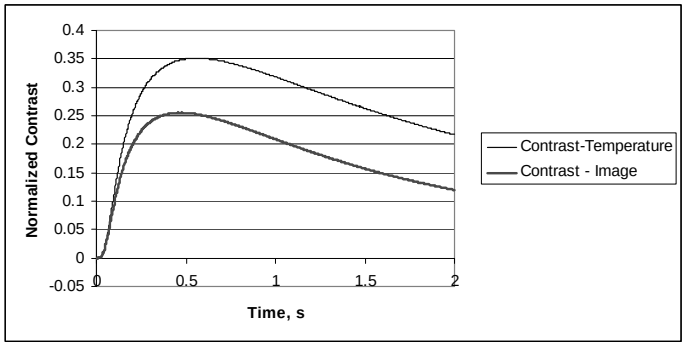

Figure 15. Comparison of estimated image contrast and simulation temperature contrast. Temperature contrast (upper curve) and image contrast (lower curve).

18. MODELING SOURCE WITH REFLECTION TEMPERATURE EVOLUTION

If we input ambient reflection temperature in a simulation model, then afterglow of the source would be due to difference in radiation between preflash and post flash reflection temperatures. The afterglow flux is given by,

$$S_{postfalsh} = \sigma\left(T_{refl}{}^{4} - T_{refl}^{0\ 4}\right) \tag{86}$$

See Fig. 16 for afterglow flux evolution.

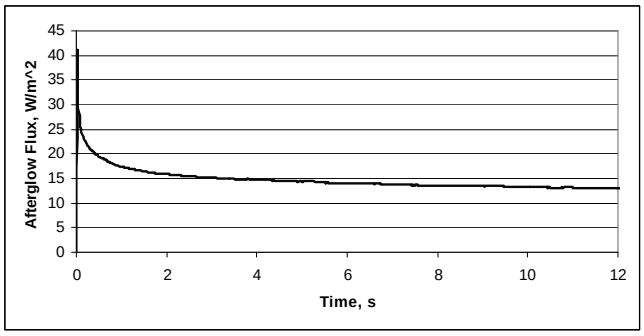

Figure 16. Afterglow flux evolution.

Afterglow flux evolution starts from first post flash frame. Flash lamp pulse flux evolution is estimated for duration between start of flash and first post flash frame. An example is shown in Fig. 17.

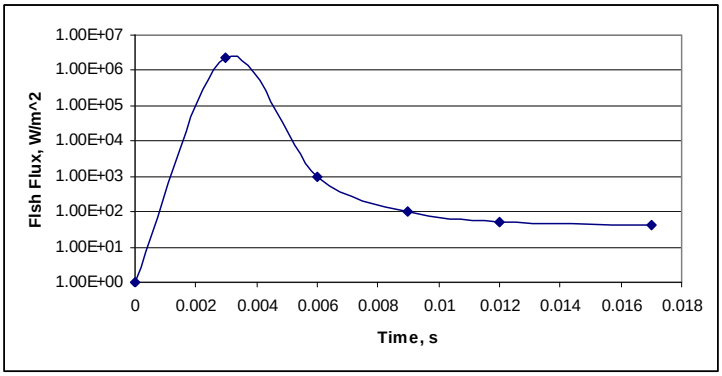

Figure 17. Flash flux evolution until first post flash frame.

Flash-lamp pulse and post flash afterglow evolutions can be added to model compound source flux evolution for duration of data acquisition time.

19. CONCLUSIONS

Normalized image contrast and normalized temperature contrast differ for objects with emissivity other than 1. Therefore, for better quantitative results the two quantities should not be treated as same. In order to compare simulation temperature contrast with measured pixel contrast, it is necessary to estimate reflection temperature evolution. It is also necessary to estimate incident heat flux. Effect of reflection temperature in pixel intensity also should be accounted to seek better estimation of temperature contrast evolution from pixel intensity evolution data.

Transient reflection temperature or reflection temperature evolution can be computed using the foil-tape technique during the flash thermography shot. Ideally, simulation should model compound heat source flux evolution which also includes thermal afterglow. We can use reflection temperature evolution to model afterglow flux of the flash source. Using estimated compound source evolution in a simulation software, we can estimate temperature contrast evolutions and then estimate image contrast evolutions on simulated voids.

The paper provides an emissivity estimation technique using flash thermography. This provides determination of emissivity for thermal wavelengths used in flash thermography set-up. If the IR cameras are programmed with the reflection temperature equations derived here, the cameras can provide object surface temperature directly, even during flash thermography data acquisition. IR cameras can be programmed to estimate the object emissivity in real-time using the formulas derived here for the foil-tape technique.

20. REFERENCES

[1] Maldague, X. P. V., "Nondestructive Evaluation of Materials by Infrared Thermography," Springer-Verlag London, (1993).
[2] Carslaw H. S. and Jaeger J. C., "Conduction of Heat in Solids," Clarendon Press, Oxford, (1959).
[3] Spicer J. W. M., "Active Thermography for manufacturing and Process Control," Short Course Notes SC05, Thermosense, SPIE – The International Society for Optical Engineering, Orlando, FL, (April 1995).
[4] Software: EchoTherm and Mosaic, Thermal Wave Imaging, Inc. Ferndale, MI, 48220, (2008).
[5] Software: ThermoFit Pro, Introscopy Institute, Tomsk, Russia, (2005).
[6] Software: ThermoCalc-3D, Introscopy Institute, Tomsk, Russia, (2005).
[7] Koshti A. M., "Estimating Temperature Rise in Pulsed Thermography using Irreversible Temperature Indicators," Proc. SPIE vol. 4702, p. 191-201, Smart Nondestructive Evaluation for Health Monitoring of Structural and Biological Systems, San Diego, CA, (March 2002).
[8] Koshti, A. M., "Methods and Systems for Characterization of an Anomaly Using Infrared Flash Thermography," U.S. Patent US8577120 B1, (Nov. 2013).
[9] Koshti A.M., "Flash Infrared Thermography Contrast Data Analysis Technique," NASA Technical report server, http://ntrs.nasa.gov, Doc. ID. 20140012757, NASA TechBriefs Webinar; Meeting Sponsor, NASA Johnson Space Center; Houston, TX, (2014).
[10] Koshti, A. M., "Infrared Contrast Analysis Technique for Flash Thermography Nondestructive Evaluation Proc. SPIE vol. 4702, p. 191-201, Smart Nondestructive Evaluation for Health Monitoring of Structural and Biological Systems, San Diego, CA, (March 2002).
[11] Koshti, A. M., "Measuring and Estimating Normalized Contrast in Infrared Flash Thermography," NASA Technical report server, http://ntrs.nasa.gov, Doc. ID: 20130009802, NASA Tech Brief, NASA Johnson Space Center; Houston, TX, United States (2013).
[12] Koshti, A. M., "Infrared contrast data analysis method for quantitative measurement and monitoring in flash infrared thermography," Structural Health Monitoring and Inspection of Advanced Materials, Aerospace, and Civil Infrastructure 2015, edited by Peter J. Shull, Proc. of SPIE Vol. 9437, 94370X-2, www.spie.org, San Diego, (April 2015).
[13] Koshti, A. M., "Methods and Systems for Characterization of an Anomaly Using Infrared Flash Thermography," Patent No. US 8,577,120 B1, (Nov. 5, 2013).
[14] Koshti, A. M., "Methods and Systems for Measurement and Estimation of Normalized Contrast in Infrared Thermography," Patent No. US 9,066,028 B1, (June 23, 2015).